



Cite this: *Polym. Chem.*, 2025, **16**, 696

Received 31st October 2024,  
Accepted 12th December 2024

DOI: 10.1039/d4py01225a

rsc.li/polymers

## Supramolecular bottlebrush copolymers from crown-ether functionalized poly(*p*-phenylenevinylene)s†

Anahita Keer, Arielle Mann, Chengyuan Wang and Marcus Weck \*

The discovery of living, chain-growth polymerizations of poly(*p*-phenylenevinylene) (PPVs) allows for low dispersed, controlled, and architecturally complex PPV-based polymers. This contribution presents the synthesis of PPVs functionalized with crown-ethers on each repeat unit that assemble with chain-end functionalized monotelechelic poly(styrene)s (PS) containing a terminal amine salt to form pseudorotaxane-based bottlebrush copolymers. The PPVs are synthesized by living ring-opening metathesis polymerization (ROMP) and the PS through atom-transfer radical polymerization (ATRP). The bottlebrush copolymer formation was confirmed by nuclear magnetic resonance spectroscopy, gel-permeation chromatography, isothermal titration calorimetry, dynamic light-scattering, wide-angle X-ray scattering, and optical spectroscopy. This work depicts the first example of a backbone modified PPV synthesized through ROMP and introduces a versatile strategy towards supramolecular bottlebrush copolymers containing conducting polymers. Our methodology lends itself to supramolecular materials for applications in chemical sensing, optoelectronics, and fluorescent imaging.

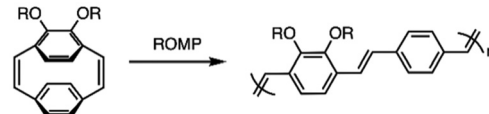
## Introduction

Organic conducting polymers, such as poly(*p*-phenylenevinylene) (PPV), are  $\pi$ -conjugated polymers with desirable optical and electrical properties.<sup>1</sup> PPVs have been used in devices such as organic light-emitting diodes (OLEDs), organic photovoltaic cells (OPVs), and as fluorescent probes in biomedical applications.<sup>2</sup> Substituting PPVs with solubilizing side-chains, such as alkoxy groups, makes this rigid-rod polymer solution processable.<sup>3</sup>

The discovery of living chain-growth polymerization of cyclophanedienes to yield PPVs using ruthenium catalysts has unlocked the development of well-defined PPV-based materials, with tuneable properties (Scheme 1).<sup>3,4</sup> [2.2] *para*-cyclophanediene (*p*Cpd) is polymerized by ring-opening metathesis polymerization (ROMP) to yield PPVs in a living, chain-growth manner with control over molecular weights, dispersities, and end-group identities.<sup>4,5</sup> The living character of ROMP also allows for the formation of block copolymers.<sup>6</sup> Recently, the Weck group reported dealkylating *para*-substituted *p*Cpds with complex side-chains that can be polymerized.<sup>7,8</sup>

Macromolecular architecture impacts polymer properties, such as packing, glassy states, melt temperatures, crystallinity, viscosity, and optical activity.<sup>9–12</sup> Bottlebrush copolymers are composed of linear polymers emanating from a main-chain, whose identity and density impacts polymer properties.<sup>13</sup> Linear PPVs have been widely reported but more complex PPV architectures are rare and PPV-based bottlebrush copolymers have not been reported to date.<sup>7,14,15</sup>

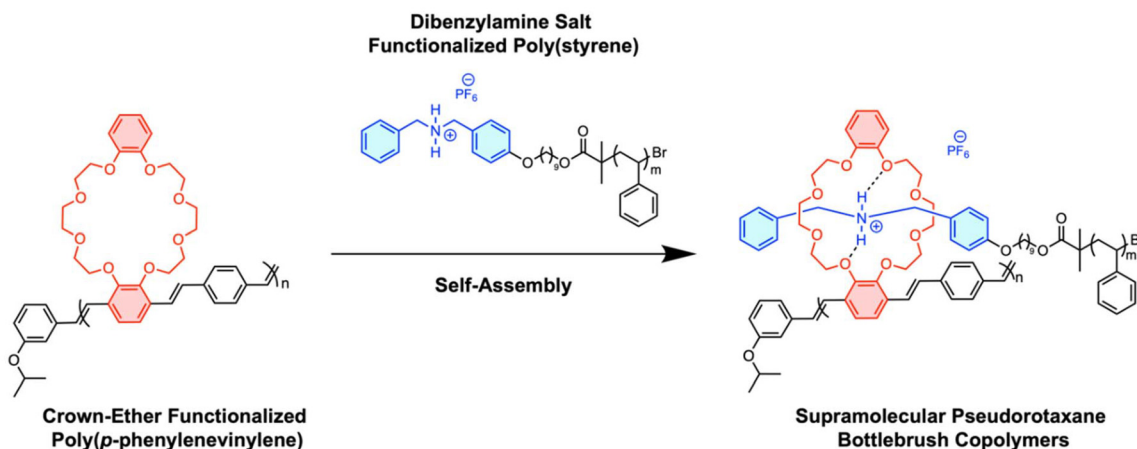
Over the past decade, to gain control over macromolecular architecture, the Weck group used molecular recognition units (MRUs) featuring noncovalent interactions such as hydrogen bonding, metal coordination, or  $\pi$ - $\pi$  stacking to directionally self-assemble polymers into complex 3D structures.<sup>16–21</sup> Macroyclic crown-ethers are prominent MRUs that form host-guest complexes with a range of both inorganic and organic cations.<sup>17,22,23</sup> Combining hydrogen bonding, coulombic interactions, electrostatic forces, and size complementarity, crown-ethers can recognize specific alkali metals and ammonium salts, resulting in the formation of pseudorotaxanes.<sup>24–26</sup> We



**Scheme 1** Ring-opening metathesis polymerization (ROMP) of *ortho*-substituted-alkoxy-[2.2] *para*-cyclophanediene. R = alkyl side-chain.

Department of Chemistry and Molecular Design Institute, New York University, New York, NY 10003, USA. E-mail: marcus.weck@nyu.edu

† Electronic supplementary information (ESI) available. See DOI: <https://doi.org/10.1039/d4py01225a>



**Scheme 2** Synthesis of supramolecular bottlebrush copolymers based on host–guest interactions between crown-ether functionalized poly(*p*-phenylenevinylene) and dibenzyl amine end-functionalized poly(styrene).

rationalize that installing crown-ethers and ammonium salts on two separate polymers, one along each repeat unit of polymer A and the other at the terminus of polymer B, supramolecular bottlebrush copolymers can be constructed (Scheme 2).<sup>18,27–29</sup>

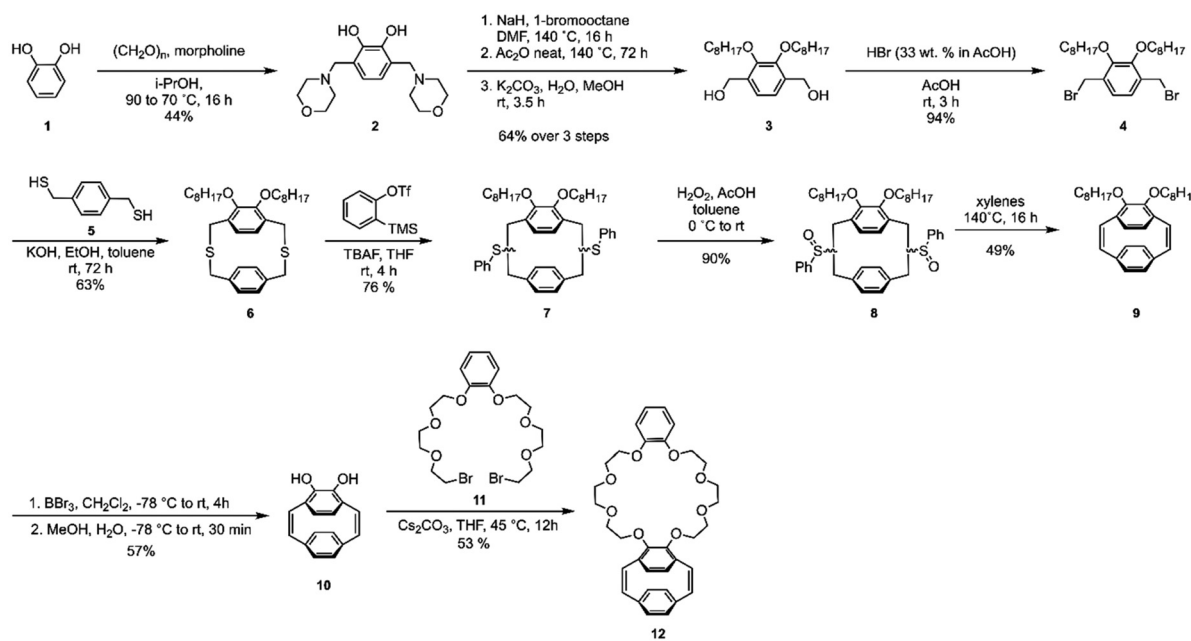
In this contribution, we report the realization of a PPV-based supramolecular bottlebrush copolymer (Scheme 2). Our design is based on *ortho*-substituted *p*Cpds appended with dibenzo-24-crown-8 (DB24C8) and polymerized *via* ROMP to afford crown-ether containing PPVs (CE-PPVs). Using atom-transfer radical polymerization (ATRP), poly(styrene) (PS) was functionalized with a complementary cationic dibenzyl ammonium ( $\text{DBA}^+$ ) at one chain-end (PS-DBA $^+$ ).<sup>30</sup> Pseudorotaxane formation yielded supramolecular bottle-

brushes which were characterized by nuclear magnetic resonance (NMR) spectroscopy, gel-permeation chromatography (GPC), isothermal titration calorimetry (ITC), dynamic light-scattering (DLS), wide-angle X-ray scattering (WAXS), and optical spectroscopy. Our work provides a platform to develop supramolecular functionalized materials for applications in areas such as sensing, optoelectronics, and fluorescent imaging.

## Results and discussion

### Synthesis

The *ortho*-substituted *p*Cpd, **9**, was synthesized in close analogy to our previous report, starting with catechol.<sup>7</sup>



**Scheme 3** Synthetic route towards CE-*p*Cpd, **12**.

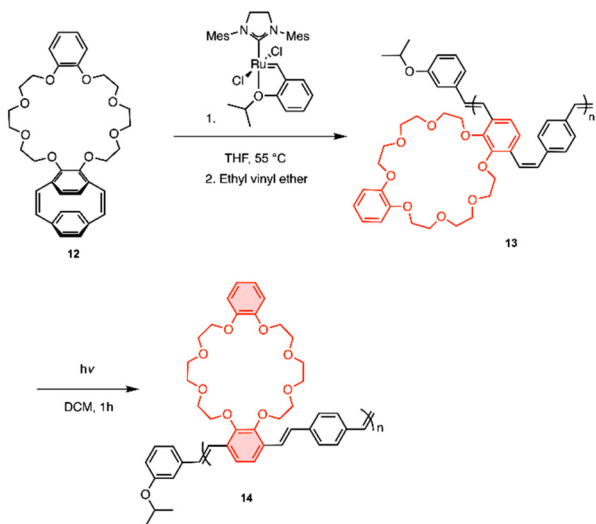
Morpholine groups were installed using a Mannich reaction. For solubility, alkoxy groups were appended and the Mannich base was exchanged over two steps to afford diol **3** which was converted to the dibromomethylated product, **4**. Under dilute conditions, **4** was reacted with **5** to form the [3.3] dithia-*para*-cyclophane **6**. Compound **6** underwent a benzene-induced Stevens rearrangement to give compound **7**, which was oxidized to form compound **8**. The sulfoxides were thermally eliminated to contract the ring resulting in diene **9**. Compound **9** was treated with boron tribromide to generate the catechol-like *p*Cpd **10**. It should be noted that when *para*-substituted *p*Cpds undergo dealkylation, the dihydroxide oxidizes to form diquinones. The same was not observed with the *ortho*-substituted *p*Cpd.<sup>31</sup> Compound **10** was reacted with dibromide **11** under basic conditions to give the desired crown-ether *p*Cpd (CE-*p*Cpd) monomer **12** (Scheme 3).

We investigated the living nature of the ROMP of **12** (Scheme 4) using Hoveyda-Grubbs' second generation initiator (HGII) (Fig. 1). All resulting polymers showed low dispersities ( $D < 1.33$ ) with full monomer consumption (Fig. 1a). We observed a linear relationship for each of the monomer to initiator feed ratios ( $[M]/[I]$ ) plotted with the molecular weights ( $M_n$ ) (Fig. 1b) (13a–d).

ROMP gives PPVs with a *cis-trans* conformation that can be photo-isomerized under UV-light to give the all-*trans*-CE-PPV, **14**. The absolute molecular weights were determined by <sup>1</sup>H NMR spectroscopy by integrating the isopropoxy protons on the initiating end-group from HGII and comparing them to the methylene protons. The livingness of the polymerization was further elucidated by preparing a diblock copolymer, which supported the presence of an active chain-end (**15**) (ESI, Scheme S2†). Again, complete monomer consumption was observed by *in situ* <sup>1</sup>H NMR spectroscopy and end-group identity by <sup>1</sup>H NMR spectroscopy and MALDI-ToF-MS (ESI, Fig. S3†). These results show that the polymerization proceeded without chain-termination or chain-transfer and the resultant polymers had low dispersities with control over polymer properties, *i.e.*, **13** was polymerized in a living, chain-grown manner.<sup>31,32</sup>

The optical properties of the PPV polymers were then investigated. Consistent with previous literature, as the molecular weight of the CE-PPVs increased, the absorbance maxima decreased while emission remained similar (Table 1).<sup>33</sup> Compared to *para*-substituted PPVs, the CE-PPVs' blue-shifted absorbance and emission wavelength maxima are consistent with *ortho*-substitution of PPVs as reported in the literature.<sup>7,33,34</sup> Previously, the Weck group published the synthesis of *ortho-para*-substituted tetra-alkoxy PPVs.<sup>7</sup> These PPVs absorb at 416 nm and emit at 524 nm, whereas the CE-PPVs absorb at 353 nm and emit at 483 nm. The substituent identity and location differ between these two PPVs. The crown-ether substituent has a significant impact on the hypsochromic shift of both optical parameters. When the *cis-trans*-CE-PPV (**13b**) photo-isomerized to the all-*trans*-**14**, the absorbance red-shifted and emission remained the same, consistent with increasing conjugation length due to lower steric crowding around the *trans* vinylene bonds (ESI, Fig. S4 and S5†).<sup>7</sup>

The second required building block towards bottle brush copolymers is a polymer containing an amine end group (Scheme 5). Monotelechelic PS was polymerized using ATRP



Scheme 4 ROMP of CE-*p*Cpd, **12**, and photo-isomerization at 395 nm.

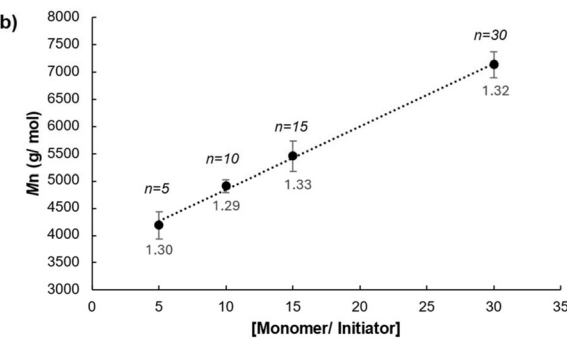
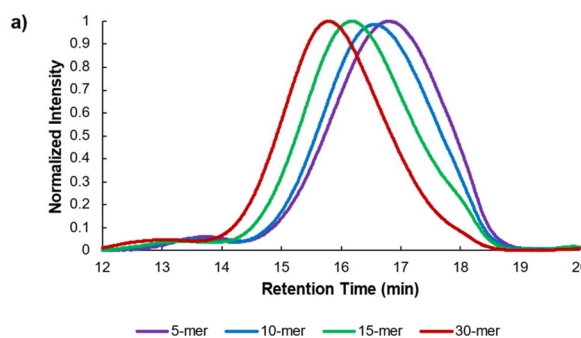
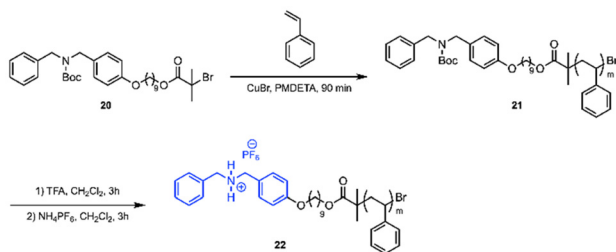


Fig. 1 (a) Molecular weight distribution of polymers **13a–d** (GPC in THF). (b) Dependence of  $M_n$  as measured by GPC of polymers **13a–d** on the  $[M]/[I]$  ratio. Here, **13a**,  $n = 5$ , **13b**,  $n = 10$ , **13c**,  $n = 15$ , and **13d**,  $n = 30$ . Dispersity values of the respective polymers are denoted in the plot.

**Table 1** GPC data and optical characterization of CE-PPVs

PPV	[M/I]	$M_n$ , Calc. <sup>a</sup>	$M_n$ , GPC <sup>b</sup>	$M_n$ , NMR <sup>c</sup>	$D$	Yield %	Abs. $\lambda_{\text{max}}$ <sup>d</sup>	Em. $\lambda_{\text{max}}$ <sup>d</sup>
13a	5	3035	4200	3035	1.30	97	361	481
13b	10	5809	4900	6483	1.29	96	353	483
13c	15	8783	5500	9357	1.33	85	349	481
13d	30 <sup>e</sup>	17 402	7150	—	1.32	83	347	482
14	10-trans	5809	6400	—	1.40	Quant.	441	482
15	Diblock <sup>e</sup>	8164	29 400	—	1.26	87	408	516

<sup>a</sup>  $M_n$  values were calculated based on the targeted degree of polymerization. <sup>b</sup>  $M_n$  GPC values were determined against poly(styrene) standards. The mobile phase was THF and the detector was UV-Vis. <sup>c</sup> The crown-ether protons of the CE-PPV were integrated against the isopropoxy proton of the end-group. <sup>d</sup> Measurements were done in dilute solutions of chloroform. <sup>e</sup> Feed ratio was too large for integration of signals.

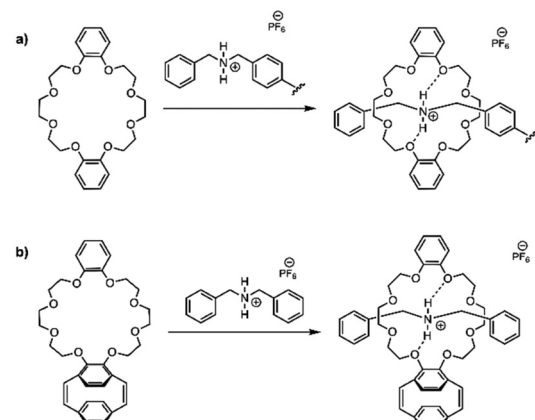
**Scheme 5** Synthesis of telechelic PS-DBA<sup>+</sup>, 22.

initiator **20** to yield polymer **21**.<sup>21,30</sup> The amine end-group was Boc-protected during the polymerization due to the presence of an amine causing uncontrolled polymerization behavior.<sup>17</sup> Trifluoroacetic acid was used to deprotect the amine and then hexafluorophosphate was added to install a non-coordinating counter-ion for the creation of the ammonium chain-end, **22**.

ATRP reached 40% conversion in four hours and was terminated to prevent any deviation from first-order kinetics.<sup>35</sup> Aliquots of the polymerization were taken every 30 minutes under an argon atmosphere. The  $M_n$  of the aliquots, analyzed by GPC, increased with time to give monomodal polymers with narrow dispersities. The semilogarithmic plot showed that ATRP progressed with first-order kinetics, which indicates a living polymerization (ESI, Fig. S6†).

### Self-assembly

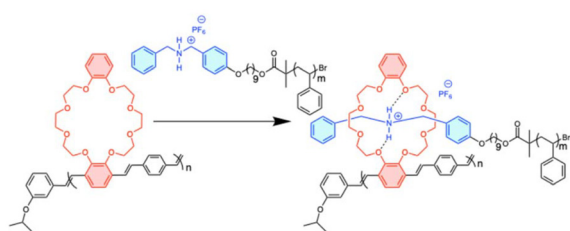
**Small molecule assemblies.** Dibenzo-24-crown-8 (DB24C8) and dibenzylammonium salt (DBA<sup>+</sup>) are known to assemble spontaneously in aprotic solvents with an association constant ( $K_a$ ) of  $1.7 \times 10^3 \text{ M}^{-1}$  in 1:1 chloroform/acetonitrile.<sup>24</sup> We first assembled commercially available DB24C8 and polymer **22**, PS-DBA<sup>+</sup> (Scheme 6a) and observed characteristic complexation using <sup>1</sup>H NMR spectroscopy (ESI, Fig. S7†). Upon addition of excess PS-DBA<sup>+</sup>, a new signal at  $\delta = 4.10 \text{ ppm}$  was observed that corresponds to “free” dibenzylammonium salt. Next, the ability of the small molecule host to form a pseudorotaxane was analyzed by complexing CE-pCpd, compound **10**, with DBA<sup>+</sup> in a 1 to 1 ratio (Scheme 6b). The characteristic methylene peaks of the crown-ether appeared between  $\delta = 3.52$  and  $4.16 \text{ ppm}$ , and the benzylic peaks of the dibenzylamine salt appears at  $\delta = 4.12 \text{ ppm}$ . The complexed methylene peaks

**Scheme 6** Pseudorotaxane formation. (a) The host is commercially available DB24C8 and the guest is PS-DBA<sup>+</sup>, **22**. (b) The host is CE-pCpd, **12**, and the guest is commercially available DBA<sup>+</sup>.

appeared at  $\delta = 4.28$ ,  $4.63$ , and  $4.94 \text{ ppm}$ . The signal at  $\delta = 4.08 \text{ ppm}$  corresponds to the salt (ESI, Fig. S8†).

**Bottlebrush copolymer assembly.** After examining the small molecule assemblies, the self-assembly of the polymeric units was investigated (Scheme 7, and Fig. 2). The guest, PS-DBA<sup>+</sup> (**22**), was titrated into the host, CE-PPV (**13b**), to form the targeted polypseudorotaxane. The host-guest complex self-assembled in a 1:1 stoichiometric equivalence ratio (based on MRUs) in a solution of 1:1 chloroform and acetonitrile, chosen to fully solubilize the cationic salt. The complexed benzylic protons appeared at  $\delta = 4.16$  to  $4.39 \text{ ppm}$  and the complexed crown-ether protons appeared from  $\delta = 3.28$  to  $3.42 \text{ ppm}$ . New signals at  $\delta = 2.78$  and  $2.55 \text{ ppm}$  represent the uncomplexed and complexed acidic ammonium cation (Fig. 2).<sup>36</sup> Upon addition of excess triethylamine, the ammonium cation was deprotonated, and the crown-ether complexation dethreaded.<sup>17</sup> The complexed ammonium peaks disappeared and the benzylic protons of the dibenzyl amine appeared at  $\delta = 3.68 \text{ ppm}$  (ESI, Fig. S9†). The polymeric bottlebrush is, therefore, pH responsive.

Due to the overlapping and broad peaks of the polymers, association constant ( $K_a$ ) was not successfully calculated through <sup>1</sup>H NMR spectroscopy, so, isothermal titration calorimetry (ITC) using 1:1 CHCl<sub>3</sub>/CH<sub>3</sub>CN as the solvent was per-



**Scheme 7** Bottlebrush copolymer assembly. The host is CE-PPV, **13b**, and the guest is PS-PBA<sup>+</sup>, **22**.

formed. PS-DBA<sup>+</sup> (**22**) was titrated into CE-PPV (**13b**) and the heat of dilution of three blanks was subtracted from the measurement. The blanks were: solvent titrated into solvent, PS-DBA<sup>+</sup> titrated into solvent, and solvent titrated into CE-PPV. The host solution had a concentration of 0.105 mM and the guest solution of 0.085 mM. The  $K_a$  was determined by a single-site binding model as  $9.305 \times 10^4 \text{ M}^{-1} \pm 1.14 \times 10^4 \text{ M}^{-1}$  and the stoichiometry ratio ( $n$ ) was found to be  $1.28 \pm 0.09$ , which is similar to the 1:1 complexation seen in the small molecule counterparts (ESI, Fig. S10†). Please note that 10 equivalents of PS-DBA<sup>+</sup> (**22**) were titrated into 1 equivalent of CE-PPV (**13b**), based on having a 10-mer host polymer with 10 CE binding sites. The polymeric units associated a magnitude of order stronger than their small molecule counterparts ( $1.7 \times 10^3 \text{ M}^{-1}$ ).<sup>24</sup> We hypothesize that this is due to the increased

$\pi$ -stacking in the conjugated PPV system compared to the reported small molecule complexes.

The changes in the hydrodynamic radius ( $R_h$ ) between CE-PPV (**13b**) and the assembled CE-PPV-PS-DBA<sup>+</sup> were characterized *via* dynamic light scattering (DLS) (Fig. 3a). The CE-PPV had an  $R_h$  of 1.5 nm with a narrow size distribution, whereas the CE-PPV-PS-DBA<sup>+</sup> had a mean  $R_h$  of 2.8 nm, with a wide size distribution. Since the pseudorotaxane was designed as a bottlebrush copolymer, there would be a high local concentration of tethered chains forced to extend away from the polymer backbone, resulting in a larger  $R_h$  and wider size distribution. The assembly was analyzed by GPC, showing a decrease in elution time and an increase in dispersity (CE-PPV  $D = 1.29$ , PS-DBA<sup>+</sup>  $D = 1.04$  and for CE-PPV-PS-DBA<sup>+</sup>  $D = 1.36$ ). This change in dispersity and retention time may indicate that a larger aggregate than the homopolymers was formed, which is most likely the bottlebrush copolymer (Fig. 3b).<sup>21</sup> It should be noted that the CE-PPV is a rigid-rod polymer while the PS-DBA<sup>+</sup> is coiled. The bottlebrush would have characteristics of both: a more coiled character than CE-PPV while being more rigid than the PS-DBA<sup>+</sup>.

Optical data of the CE-PPV (**13b**), and the bottlebrush, CE-PPV-PS-DBA<sup>+</sup> were collected in 1:1 CHCl<sub>3</sub>/CH<sub>3</sub>CN at a concentration of 0.46  $\mu$ M. In this solvent mixture, compared to chloroform only, absorbance for the CE-PPV shifted from  $\lambda_{\text{max}} = 353$  to 362 nm, and the emission shifted from  $\lambda_{\text{max}} = 482$  to 506 nm.

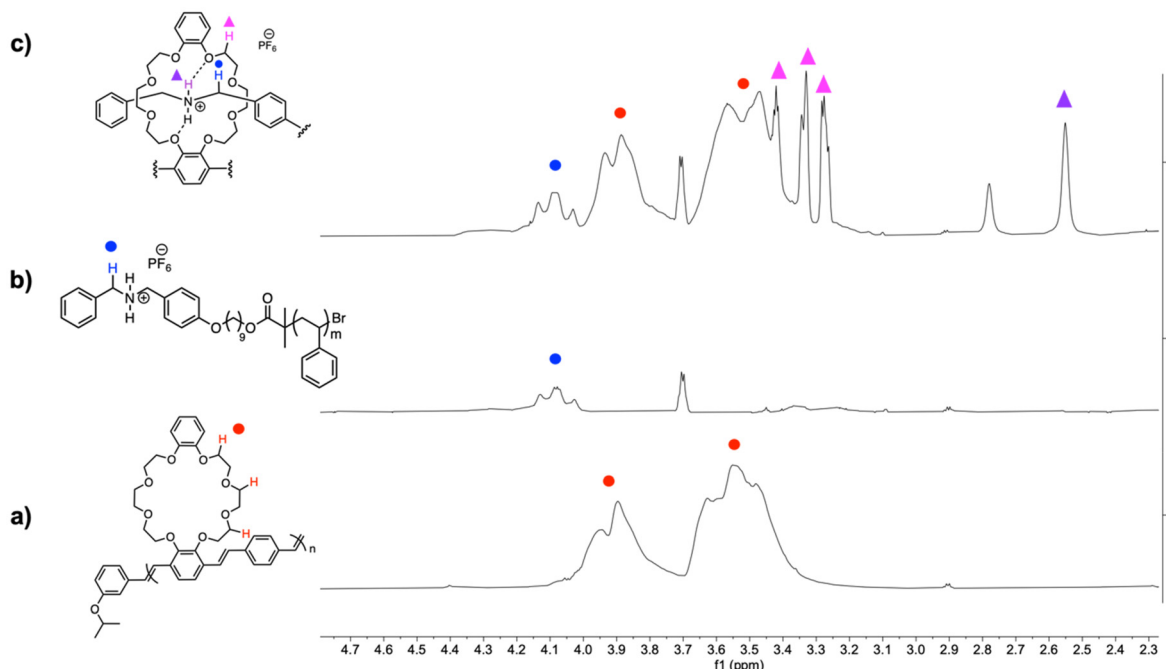


**Fig. 2**  $^1\text{H}$  NMR spectral overlay of 1.00 mM CE-PPV (**13b**) with PS-DBA<sup>+</sup> (**22**) in 1:1 CDCl<sub>3</sub>/CD<sub>3</sub>CN showing the supramolecular interaction resonances of the DBA<sup>+</sup> benzylic protons and CE protons. (a) Host–guest complex of CE-PPV and PS-DBA<sup>+</sup> in an equimolar ratio, (b) host PS-DBA<sup>+</sup> in 1:1 CDCl<sub>3</sub>/CD<sub>3</sub>CN, (c) guest CE-PPV in 1:1 CDCl<sub>3</sub>/CD<sub>3</sub>CN. The circles represent uncomplexed protons and the triangles represent complexed protons.

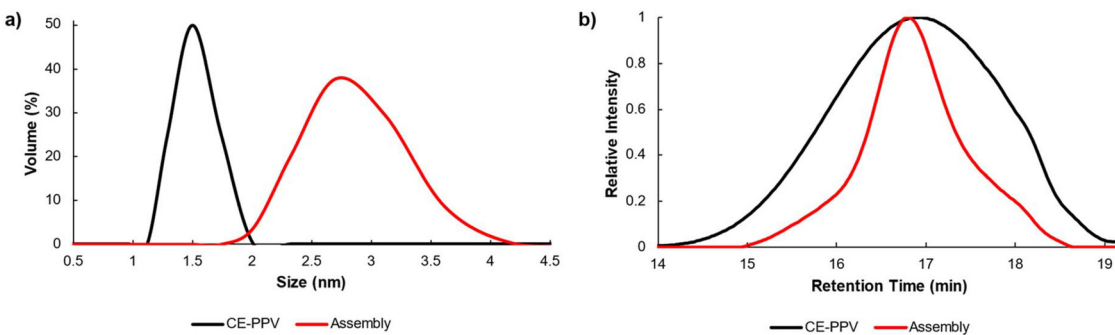


**Fig. 3** (a) DLS in 1:1  $\text{CHCl}_3/\text{CH}_3\text{CN}$  and (b) GPC characterization in THF, against linear PS standards, of homopolymer CE-PPV (**13b**) (black) and the supramolecular bottlebrush CE-PPV-PS-DBA<sup>+</sup> (red).

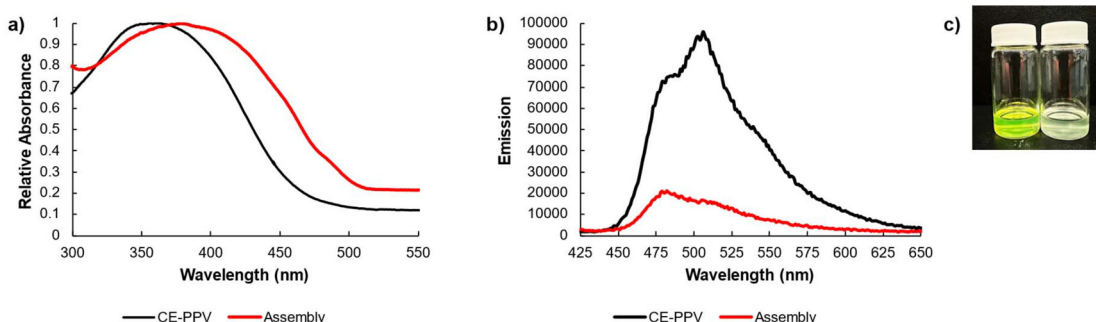


**Fig. 4** (a) Absorbance spectra and (b) emission spectra of homopolymer CE-PPV (**13b**) (black) and the supramolecular bottlebrush CE-PPV-PS-DBA<sup>+</sup> (red). (c) The CE-PPV has strong fluorescence (left) and the bottlebrush has quenched fluorescence (right).

Upon assembly, the absorbance red-shifted from  $\lambda_{\text{max}} = 362$  nm to 379 nm, which is similar to reported shifts in the literature for host–guest complexes (Fig. 4a). The emission shifted from  $\lambda_{\text{max}} = 506$  nm to 480 nm. The intensity saw a sharp, five-fold decrease in intensity from  $\sim 100\,000$  to 20 000, indicating that a guest was encapsulated into the host along the backbone (Fig. 4b). When a host–guest complex is formed in a conjugated system, the analyte (22) induced aggregation of the system elicits a quenching response (Fig. 4c).<sup>37–40</sup>

Wide-Angle X-Ray Scattering (WAXS) gave insights into the crystallinity and order of the assembled structure (Fig. 5). PPVs are known to have semi-crystalline domains that show a broad but strong scattering peak around  $2\theta = 20^\circ$ .<sup>6</sup> The CE-PPV (**13b**) spectra shows this signature peak from  $2\theta = 18$  to 21°. The Bragg's reflection at  $2\theta = 22^\circ$  corresponds to the intra-backbone repeat units, *i.e.*, the crown-ether substituent. The sharper peak could suggest that the crown-ether increases crystallinity of the CE-PPV as compared to unsubstituted or alkoxy-substituted PPVs. This may be because the crown-ether adds bulk and restricts the rotational freedom of the polymer. Features at  $2\theta = 30$ , 31, and 37° ( $d = 2.97$ , 2.88, and 2.43 Å) indicate  $\pi$ -stacking. The assembled unit does not display any short-range order features, but the peak at  $2\theta = 9.5^\circ$  corresponds to  $d = 9.30$  Å, indicating long-range order. The reflection

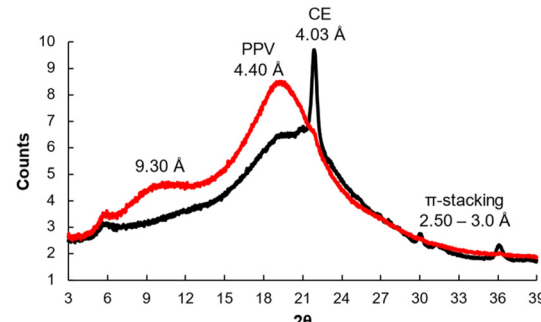


**Fig. 5** WAXS diffractograms corresponding to homopolymer CE-PPV (**13b**) (black) and the supramolecular bottlebrush CE-PPV-PS-DBA<sup>+</sup> (red).

at  $2\theta = 5.5^\circ$  was from Kapton, which held the samples during the experiment.

## Conclusions

This contribution describes a highly strained CE-*p*Cpd which, after living ROMP, yields CE-PPVs with a high degree of control over polymer properties. The living character of the

ROMP was determined by  $^1\text{H}$  NMR spectroscopy, GPC, and with chain-extension experiments. The *cis-trans*-CE-PPVs were photo-isomerized to afford the conjugated all-*trans*-isomer. PS-DBA $^+$  was synthesized using ATRP with control over molecular weights and dispersities. Brush copolymers were formed *via* the host–guest driven assembly of CE-PPV and PS-DBA $^+$ . The supramolecular bottlebrush is optically active, pH responsive, and semi-crystalline. This work depicts the first example of backbone-functionalized PPVs synthesized through ROMP and provides a platform to develop complex macromolecular architectures and supramolecular materials for applications in chemical sensing, optoelectronics, fluorescent imaging, and cross-linking.

## Data availability

The data supporting this article have been included as part of the ESI. $\dagger$

## Conflicts of interest

There are no conflicts to declare.

## Acknowledgements

The authors acknowledge financial support from the National Science Foundation under award number CHE 2203929.

## References

- 1 A. J. Heeger, *Chem. Soc. Rev.*, 2010, **39**, 2354–2371.
- 2 A. J. Blayney, I. F. Perepichka, F. Wudl and D. F. Perepichka, *Isr. J. Chem.*, 2014, **54**, 674–688.
- 3 C. Y. Yu and M. L. Turner, *Angew. Chem., Int. Ed.*, 2006, **45**, 7797–7800.
- 4 A. Mann, M. D. Hannigan and M. Weck, *Macromol. Chem. Phys.*, 2023, **224**, 2200397.
- 5 N. Zaquin, L. Lutsen, D. Vanderzande and T. Junkers, *Polym. Chem.*, 2016, **7**, 1355–1367.
- 6 E. Elacqua, G. T. Geberth, D. A. Vanden Bout and M. Weck, *Chem. Sci.*, 2019, **10**, 2144–2152.
- 7 A. Mann and M. Weck, *ACS Macro Lett.*, 2022, **11**, 1055–1059.
- 8 C. Wang, A. Mann, M. D. Hannigan, R. H. Garvey, B. L. Dumla and M. Weck, *Adv. Funct. Mater.*, 2024, **34**, 2313734.
- 9 G. Xie, M. R. Martinez, M. Olszewski, S. S. Sheiko and K. Matyjaszewski, *Biomacromolecules*, 2019, **20**, 27–54.
- 10 G. I. Peterson and T.-L. Choi, *Chem. Commun.*, 2021, **57**, 6465–6474.
- 11 E. Ahmed, C. T. Womble and M. Weck, *Macromolecules*, 2020, **53**, 9018–9025.
- 12 S. Catrouillet, L. Bouteiller, E. Nicol, T. Nicolai, S. Pensée, B. Jacquette, M. Le Bohec and O. Colombani, *Macromolecules*, 2015, **48**, 1364–1370.
- 13 S. T. Milner, *Science*, 1991, **251**, 905–914.
- 14 F. Menk, S. Shin, K.-O. Kim, M. Scherer, D. Gehrig, F. Laquai, T.-L. Choi and R. Zentel, *Macromolecules*, 2016, **49**, 2085–2095.
- 15 I. Cosemans, J. Vandenberghe, V. S. D. Voet, K. Loos, L. Lutsen, D. Vanderzande and T. Junkers, *Polymer*, 2013, **54**, 1298–1304.
- 16 R. Deng, C. Wang and M. Weck, *ACS Macro Lett.*, 2022, **11**, 336–341.
- 17 C. R. South, M. N. Higley, K. C. F. Leung, D. Lanari, A. Nelson, R. H. Grubbs, J. F. Stoddart and M. Weck, *Chem. – Eur. J.*, 2006, **12**, 3789–3797.
- 18 C. R. South, K. C. F. Leung, D. Lanari, J. F. Stoddart and M. Weck, *Macromolecules*, 2006, **39**, 3738–3744.
- 19 E. Elacqua, K. B. Manning, D. S. Lye, S. K. Pomarico, F. Morgia and M. Weck, *J. Am. Chem. Soc.*, 2017, **139**, 12240–12250.
- 20 S. K. Pomarico, D. S. Lye, E. Elacqua and M. Weck, *Polym. Chem.*, 2018, **9**, 5655–5659.
- 21 R. Deng, C. Wang, M. Milton, D. Tang, A. D. Hollingsworth and M. Weck, *Polym. Chem.*, 2021, **12**, 4916–4923.
- 22 L. Wang, L. Cheng, G. Li, K. Liu, Z. Zhang, P. Li, S. Dong, W. Yu, F. Huang and X. Yan, *J. Am. Chem. Soc.*, 2020, **142**, 2051–2058.
- 23 C. Zhang, K. Zhu, S. Li, J. Zhang, F. Wang, M. Liu, N. Li and F. Huang, *Tetrahedron Lett.*, 2008, **49**, 6917–6920.
- 24 P. R. Ashton, P. J. Campbell, P. T. Glink, D. Philp, N. Spencer, J. F. Stoddart, E. J. T. Chrystal, S. Menzer, D. J. Williams and P. A. Tasker, *Angew. Chem., Int. Ed. Engl.*, 1995, **34**, 1865–1869.
- 25 P. R. Ashton, I. Baxter, M. C. T. Fyfe, F. M. Raymo, N. Spencer, J. F. Stoddart, A. J. P. White and D. J. Williams, *J. Am. Chem. Soc.*, 1998, **120**, 2297–2307.
- 26 M. Xue, Y. Yang, X. Chi, X. Yan and F. Huang, *Chem. Rev.*, 2015, **115**, 7398–7501.
- 27 H. W. Gibson, M. A. Rouser and D. V. Schoonover, *Macromolecules*, 2022, **55**, 2271–2279.
- 28 L. He, X. Liu, J. Liang, Y. Cong, Z. Weng and W. Bu, *Chem. Commun.*, 2015, **51**, 7148–7151.
- 29 S.-J. Rao, Q. Zhang, J. Mei, X.-H. Ye, C. Gao, Q.-C. Wang, D.-H. Qu and H. Tian, *Chem. Sci.*, 2017, **8**, 6777–6783.
- 30 J.-S. Wang and K. Matyjaszewski, *J. Am. Chem. Soc.*, 1995, **117**, 5614–5615.
- 31 A. Mann, C. Wang, B. L. Dumla and M. Weck, *ACS Macro Lett.*, 2024, **13**, 112–117.
- 32 R. B. Grubbs and R. H. Grubbs, *Macromolecules*, 2017, **50**, 6979–6997.
- 33 R. P. Quirk and B. Lee, *Polym. Int.*, 1992, **27**, 359–367.
- 34 Y. Janpatompeng, A. M. Spring, V. Komanduri, R. U. Khan and M. L. Turner, *Macromolecules*, 2022, **55**, 10854–10864.
- 35 C.-Y. Yu and M. L. Turner, *Angew. Chem.*, 2006, **118**, 7961–7964.
- 36 A. Mohammad Rabea and S. Zhu, *Ind. Eng. Chem. Res.*, 2014, **53**, 3472–3477.

37 C. Wei, W. Yu, X. Liang, Y. Zhang, F. Zhang, W. Song, X. Ge, L. Wu and T. Xu, *J. Membr. Sci.*, 2022, **655**, 120580.

38 H. Liu, S. Wang, Y. Luo, W. Tang, G. Yu, L. Li, C. Chen, Y. Liu and F. Xi, *J. Mater. Chem.*, 2001, **11**, 3063–3067.

39 S. W. Thomas, G. D. Joly and T. M. Swager, *Chem. Rev.*, 2007, **107**, 1339–1386.

40 S. Wang, Y. Liu, H. Liu, G. Yu, Y. Xu, X. Zhan, F. Xi and D. Zhu, *J. Phys. Chem. B*, 2002, **106**, 10618–10621.